

Shock Tube and Modeling Study of Soot Formation during the Pyrolysis of Propane and Propane/Toluene Mixtures

G. L. Agafonov, V. N. Smirnov, and P. A. Vlasov

Semenov Institute of Chemical Physics, Russian Academy of Sciences, Kosygin str. 4, 119991
Moscow, Russia, E-mail: iz@chph.ras.ru

1 Introduction

Propane is the simplest practical hydrocarbon fuel, with its thermochemical and combustion properties being closer to those of fuels more complex than methane and ethane. Therefore, experimental and modeling studies of propane combustion with emphasis on its practical applications have drawn intense interest of researchers. To gain insights into the mechanism of soot formation during propane combustion, it seems profitable to examine its pyrolysis a constituent part of the overall oxidation accompanied by soot formation. The high temperature pyrolysis of propane was investigated using shock tube technique by a number of authors, notably Lifshitz and Frenklach [1].

The main goal of the present work is to study soot formation during pyrolysis of propane and propane/toluene mixtures both experimentally and theoretically. A further development of a detailed kinetic model of soot formation and the gas-phase mechanism of propane pyrolysis is conducted based on recently suggested concepts of PAH formation and growth, soot precursor nucleation, and the traditional surface HACA mechanism of soot particle growth.

2 Experimental Section

To obtain information for modeling the sooting behavior of propane, we performed experiments on the pyrolysis of propane/Ar and propane/toluene/Ar mixtures behind reflected shock waves over a wide temperature range. The experiments were conducted using a shock tube equipped with spectroscopic means of monitoring [2].

The parameters of the gas behind the reflected shock wave were calculated from the incident shock velocity, with the composition of the test mixture being determined based on the ideal-flow shock-tube theory. The incident wave velocity was measured with a set of three piezoelectric gauges spaced 528 and 281 mm apart, with the last one being located 40mm from the observation section. The distance from the endplate to the observation section was 15 mm. To determine the soot yield and the temperature of the soot particles, we used the double-beam absorption-emission technique.

Figure 1 shows typical absorption (frame 1) and emission (frame 2) signals. The emission signal intensity is given in relative units, in percent with respect to the signal intensity from the calibration band lamp. The time histories of the soot yield and soot temperature were calculated under the standard assumptions: the soot particles are spherical and their optical properties are described in the Rayleigh law. Triangles in frame 3 and squares in frame 4 represent the calculated soot yield and gas temperature, respectively.

The observed decay in the emission signal is associated with the arrival of the rarefaction wave at an instant of time of $\sim 1200 \mu\text{s}$; as a result, the measured temperature decreases by about 100K within the remaining $\sim 800 \mu\text{s}$ and further, by about 200 K within 2 ms; this, however, produces a minor effect on the absorption profile, since the test mixture density changes only slightly at that.

Since there is a considerable scatter in values of $E(m)$, we plotted the quantity $SY * E(m)$ as a function of time. Studying the formation of soot during the pyrolysis of toluene behind reflected shock waves, we estimated $E(m)$ as 0.37, in close agreement with the most recent data [2]. This quantity has the advantage that it was determined under conditions similar to those used in the present experiments.

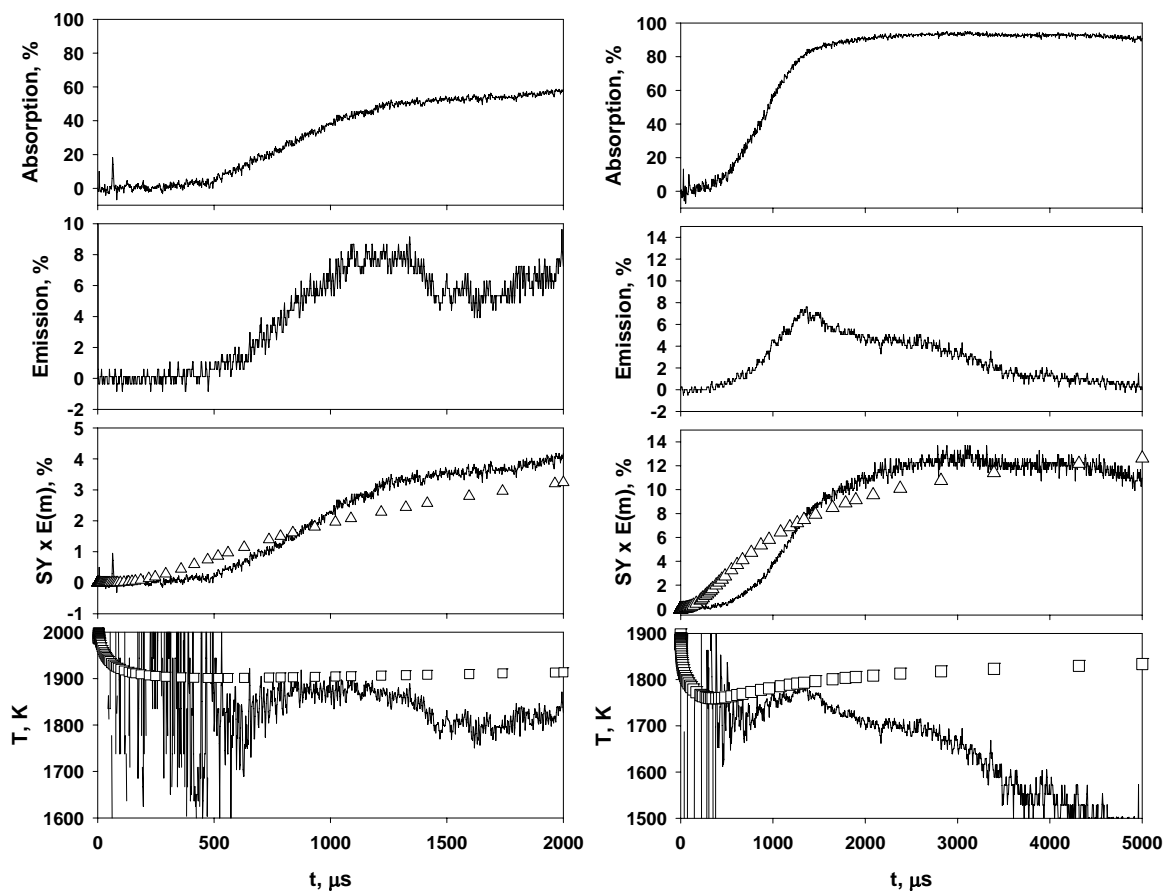


Fig. 1. Typical absorption and emission signals and the time dependences of the soot yield and temperature obtained from them for $0.0166\text{C}_3\text{H}_8 + 0.9834\text{Ar}$ (left) and $0.0145\text{C}_3\text{H}_8 + 0.001\text{Toluene} + 0.9845\text{Ar}$ (right) mixtures; initial temperatures are $T_{50} = 2297\text{ K}$ and 2085 K , correspondingly; total concentrations are $[M]_5 = 2.91 \cdot 10^{-5}$ and $3.0 \cdot 10^{-5}\text{ mol/cm}^3$, respectively; wavelength, $\lambda = 632.8\text{ nm}$. The emission signal is presented in relative units, in percent with respect to the signal from the calibration band lamp. The time evolution of the soot yield and the temperature were calculated under the standard assumptions: the soot particles are spherical and their optical properties are described by the Rayleigh formula (the particle size is much smaller than the wavelength of probing light). Triangles in frame 3 and squares in frame 4 demonstrate the calculated soot yield and gas temperature, while the lines in these frames were calculated from oscillograms given in frames 1 and 2.

3 The kinetic model

Our kinetic model postulates that the soot precursors are PAHs formed by reactions between smaller saturated PAHs and PAH radicals or between PAH radicals only. The reactions of formation of soot precursors are assumed to be irreversible. The reactions of surface growth can take place at active sites formed in reactions with hydrogen atoms. Thus, two different ensembles of soot precursors are considered in the model: soot precursors with and without active sites. Soot particles have a developed surface and each site on their surface can be activated and deactivated in the reactions with gas-phase species. At present, it is difficult to define an exact boundary between soot precursors and soot particles, but in the future, such a separation, at least formal, into several ensembles of particles may prove useful for improving the kinetic model.

The kinetic model of soot formation is based on a gas-phase reaction mechanism that describes the pyrolysis and oxidation of initial hydrocarbons, in particular methane, and the formation and growth of PAHs through different reaction pathways up to coronene. The formation, growth, oxidation, and coagulation of soot precursors and soot particles were described using the Galerkin discrete technique [2].

The core of the gas-phase reaction mechanism is the reaction sequence of PAH formation in laminar premixed acetylene and ethylene flames (HACA). At the same time, the mechanism was extended to include a number of additional channels of PAH formation and growth (up to coronene) and a comprehensive set of reactions involving C_3 -, C_5 -, and C_7 -hydrocarbons. More specifically, the mechanism included (1) the alternating H-abstraction/ C_2H_2 -addition (HACA) route, resulting in a successive growth of PAHs; (2) the combination reactions of phenyl with C_6H_6 ; (3) the cyclopentadienyl recombination; and (4) the ring-closure reactions of aliphatic hydrocarbons. The principles underlying this mechanism are outlined in [2].

The modified gas-phase reaction mechanism was comprised of 2683 direct and reverse reactions between 266 different species, with the rate coefficients of some important reactions being pressure-dependant.

Soot precursors are formed by radical-molecule reactions of different PAHs starting from phenylacetylene and ace- and ethynynaphthalene up to coronene and radical-radical reactions (from cyclopentaphenanthrene up to coronene radicals). These reactions result in the formation of polyaromatic molecules containing from 16 to 48 carbon atoms, which are stabilized by the formation of the new chemical bonds. Soot precursors are activated in reactions with H and OH radicals. They are deactivated in reactions with H, H_2 and H_2O . Soot precursors grow in reactions with C_2H_2 , C_4H_2 , and C_6H_2 , whose concentrations are rather high in pyrolysis and oxidation of aliphatic and aromatic hydrocarbons, and in reactions with polyaromatic molecules and radicals, and in coagulation. Soot precursors are oxidized by O and OH radicals. They are transformed into soot particles in the reactions of internal conversion, in which the number of active sites in the reacting system is preserved. Soot particles with active sites grow in the reactions with C_2H_2 , C_4H_2 , C_6H_2 and PAH molecules and radicals. All types of soot particles participate in coagulation.

3 Results and discussion

The results of comparison of experimentally measured in [1] and calculated product distribution in shock tube pyrolysis of $0.016C_3H_8 + 0.984Ar$ mixture are presented in Fig. 2.

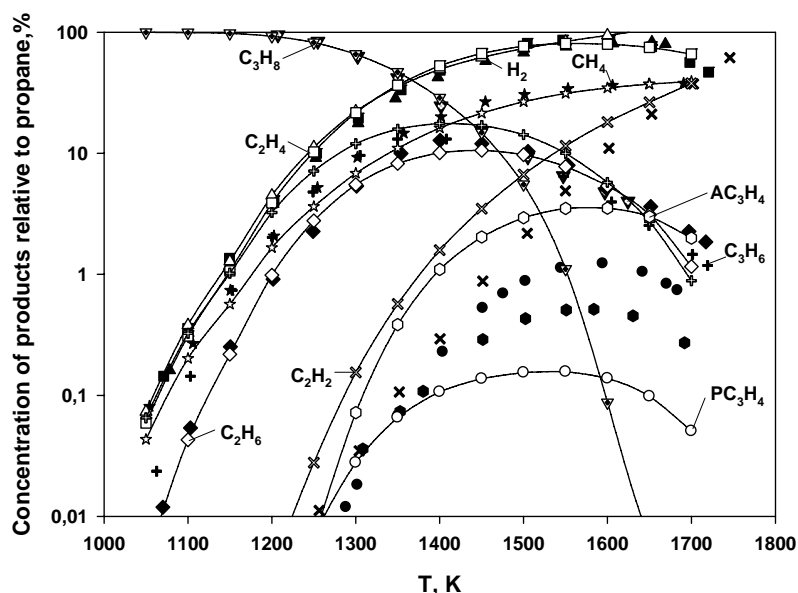


Fig. 2. Product distribution in shock tube pyrolysis of a $0.016C_3H_8 + 0.984Ar$ mixture (the initial pressure $p_1 = 0.26$ bar, $p_5 = 7$ bar). Closed symbols designate the experimental results reported in [1]. Open symbols designate the results of our calculations.

The experimentally measured and calculated temperature dependences of the soot yield during pyrolysis of different propane/Ar and propane/toluene/Ar mixtures are shown in Fig. 3. A synergetic effect of toluene additives to the propane/Ar mixture is obvious.

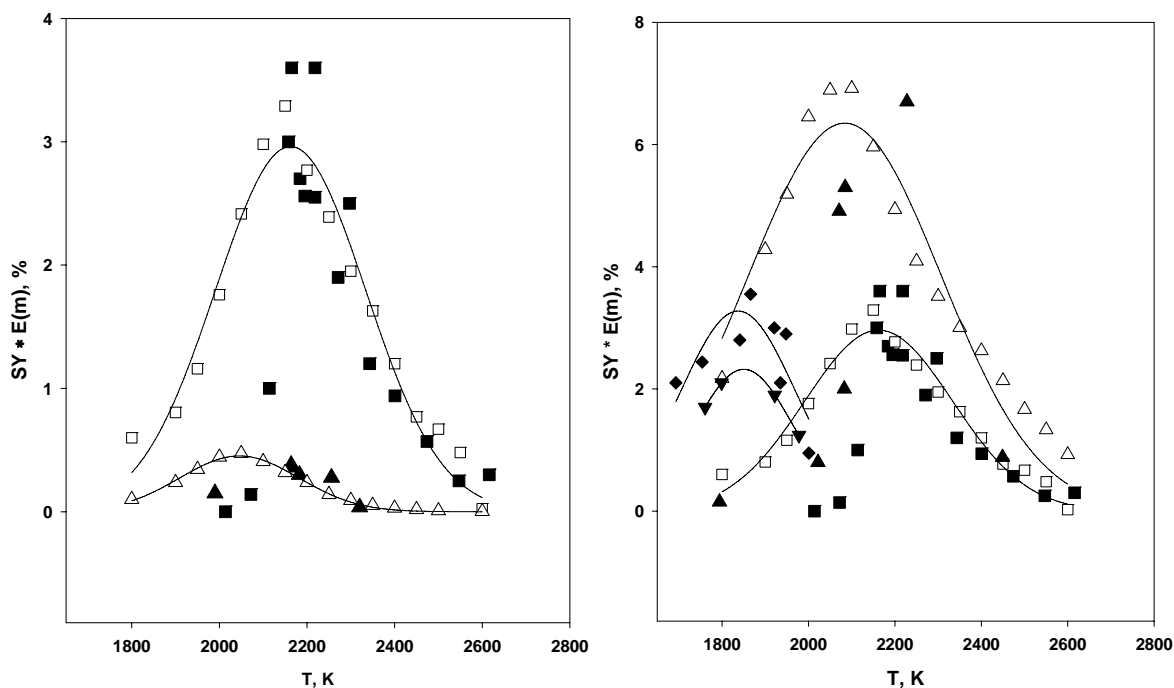


Fig. 3. Temperature dependences of the soot yield for the shock-tube pyrolysis of various propane/Ar (left) and different toluene/Ar, propane/Ar, and propane/toluene/Ar (right) mixtures. The left plot: (triangles) $0.0083\text{C}_3\text{H}_8 + 0.9917\text{Ar}$, $p_{50} = 5$ bar, (squares) $0.0166\text{C}_3\text{H}_8 + 0.9834\text{Ar}$, $p_{50} = 5.5$ bar. The right plot: (inverted triangles) $0.00097\text{toluene} + 0.99903\text{Ar}$, $p_{50} = 5$ bar, (diamonds) $0.00108\text{toluene} + 0.99892\text{Ar}$, $p_{50} = 5$ bar, (squares) $0.0166\text{C}_3\text{H}_8 + 0.9834\text{Ar}$, $p_{50} = 5.5$ bar, (triangles) $0.0145\text{C}_3\text{H}_8 + 0.001\text{toluene} + 0.9845\text{Ar}$, $p_{50} = 5.5$ bar. Closed symbols designate the results of our experiments and open symbols designate the results of our calculations. $E(m) = 0.37$.

4 Conclusions

The experiments on the pyrolysis of propane/Ar and propane/toluene/Ar mixtures behind reflected shock waves aimed on measuring the soot yield and the soot particle temperature demonstrated that there is a pronounced maximum in the temperature dependence of the soot yield and that the position and height of this peak are strongly dependent on the propane concentration and the amount of toluene additive. The proposed detailed kinetic model adequately describes the experimental results.

References

- [1] Lifshitz A and Frenklach M. (1975). Mechanism of the High Temperature Decomposition of Propane. The Journal of Physical Chemistry. **79**(7):686-692
- [2] Agafonov GL, Borisov AA, Smirnov VN, Troshin KYa, Vlasov PA, Warnatz J. (2008). Soot Formation during Pyrolysis of Methane and Rich Methane/Oxidation Mixtures behind Reflected Shock Waves. Combustion Science and Technology. **180**(10): 1876-1899